



# A novel synthesis of Ni<sub>2</sub>P/MCM-41 catalysts by reducing a precursor of ammonium hypophosphite and nickel chloride at low temperature

Hua Song<sup>a,b,\*</sup>, Min Dai<sup>a,d</sup>, Hualin Song<sup>c,\*\*</sup>, Xia Wan<sup>a,d</sup>, Xiaowei Xu<sup>a</sup>

<sup>a</sup> College of Chemistry & Chemical Engineering, Northeast Petroleum University, Daqing 163318, China

<sup>b</sup> Provincial Key Laboratory of Oil & Gas Chemical Technology, College of Chemistry & Chemical Engineering, Northeast Petroleum University, Daqing 163318, Heilongjiang, China

<sup>c</sup> Department of Image College Mudanjiang Medical University, Mudanjiang 157011, Heilongjiang, China

<sup>d</sup> CPE Survey and Design Institute of Xinjiang Oil, Karamay 834000, Xinjiang, China



## ARTICLE INFO

### Article history:

Received 8 January 2013

Received in revised form 23 April 2013

Accepted 12 May 2013

Available online 20 May 2013

### Keywords:

Nickel phosphide

Ammonium hypophosphite

Nickel chloride

MCM-41

Hydrodesulfurization

Dibenzothiophene

## ABSTRACT

A novel method to prepare Ni<sub>2</sub>P/MCM-41 catalysts at low reduction temperature based on ammonium hypophosphite and nickel chloride by temperature programmed reduction is described. The catalysts were prepared using incipient wetness impregnation of the siliceous MCM-41 support with aqueous solutions of ammonium hypophosphite and nickel chloride, followed by reducing the obtained precursor at 483–663 K for 2 h in flowing H<sub>2</sub>, to form Ni<sub>2</sub>P catalysts. The catalysts were characterized by H<sub>2</sub> temperature-programmed reduction (H<sub>2</sub>-TPR), X-ray diffraction (XRD), N<sub>2</sub>-adsorption specific surface area measurements (BET), CO uptake, transmission electron microscope (TEM), and X-ray photoelectron spectroscopy (XPS). With sample of initial P/Ni molar ratio >0.5, the Ni<sub>2</sub>P was successfully obtained at lower reduction temperature, and a high initial P/Ni molar ratio favors the formation of Ni<sub>2</sub>P at lower temperature. Using less oxidic phosphorus precursor of hypophosphite enabled the Ni<sub>2</sub>P to be formed at low reduction temperature. Evaluation of the activity for DBT HDS of the catalysts shows that the catalyst prepared with initial P/Ni ratios of 2 exhibited the highest activity. At a reaction temperature of 613 K, a pressure of 3.0 MPa, a H<sub>2</sub>/oil ratio of 500 (V/V), and a weight hourly space velocity (WHSV) of 2.0 h<sup>-1</sup>, the HDS conversion reached 99%, and no catalyst deactivation was observed within 120 h.

© 2013 Elsevier B.V. All rights reserved.

## 1. Introduction

Driven by the growing demand for fuel oil and the increasing use of heavy crude oil, sulfur removal from fuels has received and will continue to attract much attention in the coming years. Moreover, more and more rigorous environmental regulations limiting the emissions of sulfur dioxide and the continuing decline in the quality of petroleum feedstocks have made sulfur removal becomes one of the paramount problems in the refining industry. To solve these low levels of sulfur, much of the research over the past decade has aimed at improving the classic catalysts, which are based on molybdenum sulfide and promoted with cobalt or nickel, as well as finding new catalyst materials [1–4].

In recent years, transition metal phosphides, which have high activity and stability, have been found to be quite promising as

alternative hydrodesulfurization catalysts [5,6]. Among the phosphides, nickel phosphide (Ni<sub>2</sub>P) shows excellent activity for the hydrotreatment of fuels [7,8]. All recent reports of Ni<sub>2</sub>P catalysts were mostly produced by temperature programmed reduction (TPR) of metal nickel salt together with ammonium phosphate in hydrogen [5,9,10]. The nickel phosphate precursor is prepared mainly by impregnation of the support with (NH<sub>4</sub>)<sub>2</sub>HPO<sub>4</sub> (or NH<sub>4</sub>H<sub>2</sub>PO<sub>4</sub>) and Ni(NO<sub>3</sub>)<sub>2</sub> solutions, then dried and calcined. After a subsequent temperature programmed reduction in hydrogen, the desired Ni<sub>2</sub>P catalyst is formed. The method of temperature programmed reduction is convenient and simple, but has the disadvantage of requiring a high reduction temperature. Berhault et al. [11] had observed that the phosphate reduction to phosphide did not start until the reduction temperature is raised to 823 K and the selective formation of Ni<sub>2</sub>P phase begins at reduction temperature of 923 K. The P–O bond is strong, and its reduction requires high temperature. Moreover, hydrogen atoms are available only after metal nickel particles have formed, because the nickel particles are necessary for hydrogen molecules dissociating to hydrogen atoms [1]. These active hydrogen atoms can spill over to the phosphate and reduce it to phosphorus or phosphine. The phosphorus or phosphine can then react with the metal particles to form Ni<sub>2</sub>P. The strong P–O bond and the surface diffusion

\* Corresponding author at: College of Chemistry & Chemical Engineering, Northeast Petroleum University, Daqing 163318, China. Tel.: +86 0459 6503167; fax: +86 0459 6506498.

\*\* Corresponding author. Tel.: +86 0453 6984321; fax: +86 0453 6586656.

E-mail addresses: [songhua2004@sina.com](mailto:songhua2004@sina.com) (H. Song), [songhualin@126.com](mailto:songhualin@126.com) (H. Song).

of the H atoms are responsible for the high reduction temperature which leads to larger catalyst particles, relatively low catalytic activity and the almost exclusive formation of phosphorus [1]. There have been other approaches to preparing Ni<sub>2</sub>P catalysts, such as solvothermal reactions [12–16], thermal decomposition of nickel thiophosphate (NiPS<sub>3</sub>) [17], mixing of trioctylphosphine (TOP) with metal salts [18–23], and co-reaction of metal or metal oxide with phosphines [1]. However, the need for extreme conditions has limited all these approaches. Recently, it has been reported that the Ni<sub>2</sub>P were prepared by thermal decomposition of hypophosphites in a static protecting gas atmosphere [24–28]. This route is mild and does not require a high temperature. Moreover, Cecilia and Infantes-Molina found the formation of Ni<sub>2</sub>P also can be achieved by temperature-programmed reduction of phosphite-based precursors (Ni(HPO<sub>3</sub>H)<sub>2</sub>) at a relatively low temperature [29,30]. In general, using the hypophosphites as phosphorus sources provides a new method to prepare Ni<sub>2</sub>P catalyst under mild conditions.

In this paper, we demonstrate a method for preparing Ni<sub>2</sub>P/MCM-41 catalysts at lower reduction temperature. The catalyst precursors were prepared by impregnation of an ammonium hypophosphite and nickel chloride solution with MCM-41 support, followed by reduction of the precursors in a flow of H<sub>2</sub> at 483–663 K for 2 h, to obtain the Ni<sub>2</sub>P catalysts. Compared with preparation of the catalyst using the conventional TPR method, these conditions are mild because the reduction temperature has decreased by about 200 K.

## 2. Experimental

### 2.1. Catalyst synthesis

Siliceous MCM-41 was synthesized using tetraethyl orthosilicate (TEOS) as the silica source and cetyltrimethylammonium bromide (CTAB) as the template, following the procedure as described in the literature [31].

The supported Ni<sub>2</sub>P catalyst precursors were prepared by impregnating an ammonium hypophosphite (NH<sub>4</sub>H<sub>2</sub>PO<sub>2</sub>) and nickel chloride (NiCl<sub>2</sub>·6H<sub>2</sub>O) solution with the mesoporous MCM-41. The precursors, with different initial P/Ni molar ratios (0.5, 1, 2, and 3), were prepared with Ni loading of 12 wt%. In a typical experiment, 4.0 g NH<sub>4</sub>H<sub>2</sub>PO<sub>2</sub> and 5.9 g NiCl<sub>2</sub>·6H<sub>2</sub>O were dissolved in 20 mL of deionized water at room temperature to form a uniform solution (the initial molar ratio of P/Ni is 2). The MCM-41 was wet-impregnated with the above solution for 8 h. After evaporation of water, the impregnated solid was dried at 333 K and then directly reduced in a fixed-bed reactor by heating to 483–663 K at a rate of 2 K/min in a flow of H<sub>2</sub> (200 mL/min), held for 2 h, then naturally cooled to room temperature in a continuous H<sub>2</sub> flow. The obtained catalyst was passivated in O<sub>2</sub>/N<sub>2</sub> mixture (0.5 vol.% of O<sub>2</sub>) with flowrate of 20 mL/min for 2 h. The precursors obtained before reducing and catalysts were named NiCl<sub>2</sub>-NH<sub>4</sub>H<sub>2</sub>PO<sub>2</sub>/MCM(X) and Ni-P/MCM(X-Y), respectively, where X and Y are the initial P/Ni molar ratio and reduction temperature, respectively.

### 2.2. Catalyst characterization

The reducibility of precursors was characterized by the H<sub>2</sub> temperature-programmed reduction (H<sub>2</sub>-TPR) using a quartz U-tube reactor (inner diameter of 6 mm), in which 0.05 g of catalyst was loaded in the thermostatic zone. Reduction was conducted at a heating rate of 10 K/min in a 10 vol.% H<sub>2</sub>/Ar flow (30 mL/min). The TPR spectrum was determined using a thermal conductivity detector (TCD) to monitor hydrogen consumption.

X-ray diffraction (XRD) analysis of the samples were carried out on a D/max-2200PC-X-ray diffractometer using CuK $\alpha$  radiation

under the setting conditions of 40 kV, 30 mA, scan range from 10 to 80° at a rate of 10°/min.

The typical physico-chemical properties of supports and catalysts were analyzed by BET method using Micromeritics adsorption equipment of NOVA2000e. All the samples were outgassed at 473 K until the vacuum pressure was 6 mm Hg. The adsorption isotherms for nitrogen were measured at 77 K.

Transmission electron microscope (TEM) examinations were performed using the JEM-1010 instrument supplied by JEOL. The samples were dispersed in ethanol and placed on a carbon grid before TEM examinations.

The CO uptake was measured using pulsed chemisorption. About 1.0 g of catalyst was pretreated in a quartz reactor to remove the passivation layer by heating up to 613 K at a rate of 2 K/min in H<sub>2</sub> with flowrate of 20 mL/min for 2 h, and then naturally cooled to room temperature in a continuous H<sub>2</sub> flow and an He flow at 30 mL/min was used to flush the catalyst for 30 min to achieve an adsorbate-free. After pretreatment, 1 mL pulses of CO were injected into a flow of He (30 mL/min), and the CO uptake was measured using a TCD. CO pulses were repeatedly injected until the response from the detector showed no further CO uptake after consecutive injections. Assuming a 1:1 adsorption stoichiometry between CO and metal atoms, this value corresponds to the metal site density on the catalyst surface.

The X-ray photoelectron spectroscopy (XPS) spectra were acquired using ESCALAB MKII spectrometer under vacuum. XPS measurements have been performed using monochromatic Mg K $\alpha$  radiation ( $E = 1253.6$  eV) and equipped with a hemi-spherical analyzer operating at fixed pass energy of 40 eV. The recorded photoelectron binding energies were referenced against the C 1s contamination line at 284.8 eV.

### 2.3. Catalytic activity test

The HDS of DBT was carried out in a flowing high-pressure fixed-bed reactor using a feed consisting of a decalin solution of DBT (1 wt%). The conditions of the HDS reaction were 553–613 K, 3.0 MPa, WHSV = 2 h<sup>-1</sup>, and hydrogen/oil ratio of 500 (V/V). The catalyst was pressed in discs, crushed and sieved with 30–60 mesh. Prior to reaction, 0.5 g of the catalysts were pretreated in situ with flowing H<sub>2</sub> (40 mL/min) at 613 K for 2 h. Sampling of liquid products was started 6 h after the steady reaction conditions had been achieved. Liquid samples were collected every hour and analyzed by FID gas chromatography with a GC-<sup>14</sup>C-<sup>60</sup> column. The total conversion was calculated from the ratio of converted dibenzothiophene/initial dibenzothiophene. Turnover frequency (TOF) values of the samples containing nickel phosphide were calculated using Eq. (1) [32]:

$$\text{TOF} = \frac{F}{W} \frac{X}{M} \quad (1)$$

where F is the molar rate of DBT fed into the reactor (μmol s<sup>-1</sup>), W is the weight of catalyst (g), X is the conversion of DBT (%), and M is the mole of sites loaded which is decided by the CO uptake.

## 3. Results and discussion

### 3.1. H<sub>2</sub>-TPR analysis

H<sub>2</sub>-TPR profiles of MCM-41-supported NiCl<sub>2</sub>, NH<sub>4</sub>H<sub>2</sub>PO<sub>2</sub> and catalyst precursors with different initial P/Ni molar ratios are shown in Fig. 1. With sample (a) (NiCl<sub>2</sub>/MCM), the hydrogen consumption peak attributed to the reduction of Ni<sup>2+</sup> to Ni is observed around 640 K, while with sample (b) the peaks were weaker, and then which is hardly observed with increasing P content (samples (c)–(d)). This indicates that the P content in the precursor

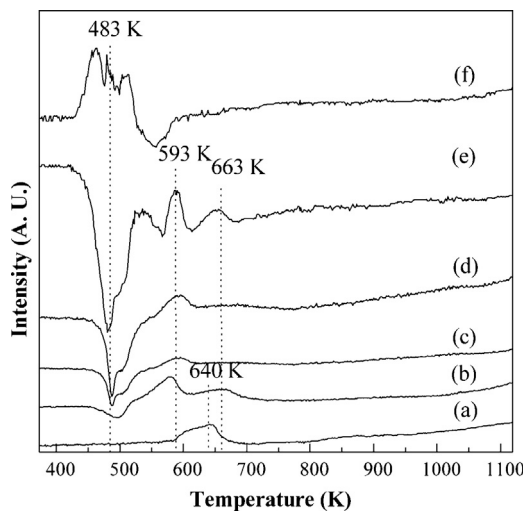


**Fig. 1.**  $\text{H}_2\text{-TPR}$  profiles of MCM-41 supported  $\text{NiCl}_2$ ,  $\text{NH}_4\text{H}_2\text{PO}_2$ , and  $\text{NiCl}_2\text{-NH}_4\text{H}_2\text{PO}_2/\text{MCM}(X)$ . (a)  $\text{NiCl}_2$ , (b)  $\text{P}/\text{Ni} = 0.5$ , (c)  $\text{P}/\text{Ni} = 1$ , (d)  $\text{P}/\text{Ni} = 2$ , (e)  $\text{P}/\text{Ni} = 3$ , (f)  $\text{NH}_4\text{H}_2\text{PO}_2$ .

has a great effect on the reduction of  $\text{Ni}^{2+}$  to Ni by  $\text{H}_2$ . For samples (b)–(e) ( $\text{NiCl}_2\text{-NH}_4\text{H}_2\text{PO}_2/\text{MCM}(X)$ ), some significant negative peaks are found at about 483 K, this maybe due to some gas (such as  $\text{HCl}$  and  $\text{NH}_3$ ) has been produced during the heating process, and therefore the TCD appears a negative signal opposite of  $\text{H}_2$  consumption. These negative peaks correspond to the decomposition of the precursors. However, the sample (f) ( $\text{NH}_4\text{H}_2\text{PO}_2/\text{MCM}$ ) shows a hydrogen consumption peak around 483 K, which indicates that phosphorus species come from the decomposition of  $\text{NH}_4\text{H}_2\text{PO}_2$  can be reduced at low temperature. Hydrogen consumption peaks with samples (b)–(e) attributed to the reduction of phosphorus species is observed around 593 K, which is higher than that observed in the sample (f). This indicates that in the catalyst precursors, the nickel is likely to be in the form of hypophosphite and reaction occurs at the intrinsic reduction temperature of this main hypophosphite phase. The sample (b)–(e) also show the  $\text{H}_2$  consumption decrease with the increase in phosphorous loadings. Moreover, some weak peaks of  $\text{H}_2$  consumption appeared at about 663 K, which indicates that a small amount of phosphorous species has been reduced.

It has been reported that the reduction of  $\text{Ni}_2\text{P}$  from a precursor prepared by  $(\text{NH}_4)_2\text{HPO}_4$  (or  $\text{NH}_4\text{H}_2\text{PO}_4$ ) and  $\text{Ni}(\text{NO}_3)_2$  do not occur until the temperature reaches 823 K [11]. Such a high reduction temperature is attributed to the highly thermodynamic stability of P–O bond and the surface diffusion of the H atoms [1]. But our  $\text{H}_2\text{-TPR}$  analysis shows that compare with the precursor prepared by  $(\text{NH}_4)_2\text{HPO}_4$  (or  $\text{NH}_4\text{H}_2\text{PO}_4$ ) and  $\text{Ni}(\text{NO}_3)_2$ , the reduction of  $\text{Ni}_2\text{P}$  from a precursor prepared by  $\text{NiCl}_2$  and  $\text{NH}_4\text{H}_2\text{PO}_2$  could be performed at a lower temperature. The reduction temperature has decreased by about 200 K. This may be due to the P species with less valence electron can be easily reduced, because P in  $\text{NH}_4\text{H}_2\text{PO}_2$  has one valence electron, which is four less than that of P in  $(\text{NH}_4)_2\text{HPO}_4$  (or  $\text{NH}_4\text{H}_2\text{PO}_4$ ). Our method which use less oxidic phosphorus precursor of hypophosphite enables the  $\text{Ni}_2\text{P}$  to be formed at even lower reduction temperature. These observations are similar to the results reported by Cho et al. [16].

### 3.2. XRD

In order to optimize the experimental conditions to obtain the desired  $\text{Ni}_2\text{P}$  phase, the influence of the initial P/Ni molar ratio and reduction temperature on the formation of  $\text{Ni}_2\text{P}$  were studied. The XRD patterns of the samples with initial P/Ni ratios of 0.5, 1, 2, and

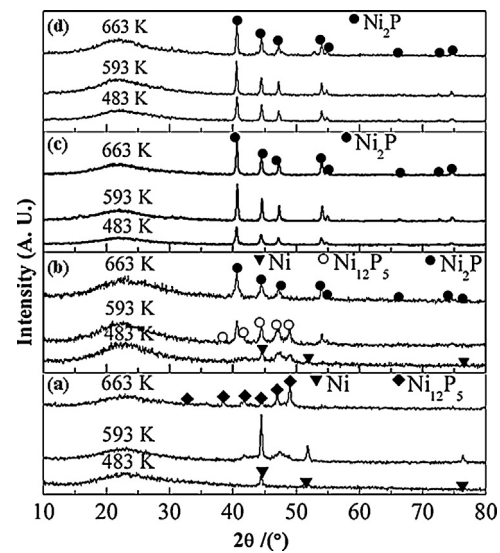


**Fig. 2.** XRD patterns of the catalysts prepared with different initial Ni/P molar ratios and reduced at different temperature. (a)  $\text{P}/\text{Ni} = 0.5$ , (b)  $\text{P}/\text{Ni} = 1$ , (c)  $\text{P}/\text{Ni} = 2$ , (d)  $\text{P}/\text{Ni} = 3$ .

3 reduced at 483, 593 and 663 K are presented in Fig. 2. All the patterns show a broad feature at  $2\theta = 25^\circ$  due to the amorphous nature of mesoporous MCM-41 [29]. As shown in Fig. 2(a) (initial P/Ni molar of 0.5), Ni phase is detected at 44.4, 51.8, and 76.7° (PDF: 65–2865) with sample reduced at 483 K. When the temperature rises above 593 K, the intensity of Ni phase increased and an amorphous  $\text{Ni}_{12}\text{P}_5$  phase formed. When the temperature is up to 663 K, the Ni phase disappeared, and the  $\text{Ni}_{12}\text{P}_5$  phase is detected at 32.6, 35.8, 38.4, 41.7, 44.4, 46.9 and 48.9° (PDF: 22–1190). The situation is somewhat different when the initial P/Ni molar ratio increased. With initial P/Ni molar of 1 (Shown in Fig. 2(b)), Ni phase and amorphous  $\text{Ni}_{12}\text{P}_5$  phase are detected at 483 K, and both Ni phase and  $\text{Ni}_{12}\text{P}_5$  phase are observed at 593 K. With the temperature rises to 593 K, the  $\text{Ni}_2\text{P}$  phase is detected at 40.6, 44.5, 47.1, 54.1, 54.8, 66.1, 72.5 and 74.5° (PDF: 03–0953) at 663 K. With initial P/Ni molar of 2 and 3 (Fig. 2(c) and (d)), the pure  $\text{Ni}_2\text{P}$  phase is detected, and the peak intensity increases with the reduction temperature increased from 483 to 593 K and then maintains the intensity with the reduction temperature up to 663 K. The XRD analysis results show that formation of active phases follows the order Ni,  $\text{Ni}_{12}\text{P}_5$  and  $\text{Ni}_2\text{P}$ , which coincides with the previously published studies [33].  $\text{Ni}_2\text{P}$  was not obtained for sample prepared with initial P/Ni molar of 0.5, probably because of lack of P and partial loss of P due to the formation of  $\text{PH}_3$  or P during reducing process. Prins et al. [34] have pointed out the possibility for formation of volatile species such as elemental P or phosphine ( $\text{PH}_3$ ) during the reduction processes, and then the formed  $\text{PH}_3$  reacts with nickel to form Ni,  $\text{Ni}_{12}\text{P}_5$  or  $\text{Ni}_2\text{P}$  phase [35]. At temperature of 483 K, greater proportions of  $\text{PH}_3$  is formed by the decomposition of phosphorous rich precursors and react with nickel particles to form phosphorous rich phosphides such as  $\text{Ni}_{12}\text{P}_5$  and  $\text{Ni}_2\text{P}$ . With temperature increases to 593 K, the  $\text{Ni}_{12}\text{P}_5$  phase transforms to  $\text{Ni}_2\text{P}$  phase for the sample with initial P/Ni molar ratio of 1 and the peaks of  $\text{Ni}_2\text{P}$  phase become more intense for the samples with initial P/Ni molar ratio of 2 and 3, indicating  $\text{PH}_3$  was formed at this temperature again, and which promoted the formation of  $\text{Ni}_2\text{P}$  phase. At temperature of 663 K,  $\text{Ni}^{2+}$  can be reduced by  $\text{H}_2$ , and then which is reduced to  $\text{Ni}_{12}\text{P}_5$  or  $\text{Ni}_2\text{P}$ . Therefore, the advantage of using  $\text{NiCl}_2$  and  $\text{NH}_4\text{H}_2\text{PO}_2$  as materials to prepare  $\text{Ni}_2\text{P}$  is that the synthesis process can be carried out under a relative low reduction temperature.

**Table 1**

Textural characterization of support and catalysts.

Sample	BET area (m <sup>2</sup> g <sup>-1</sup> )	Pore volume (cm <sup>3</sup> g <sup>-1</sup> )	Average pore diameter (nm)
MCM-41	1012	0.816	3.2
Ni-P/MCM(0.5–483)	507	0.363	2.8
Ni-P/MCM(0.5–663)	815	0.584	2.9
Ni-P/MCM(1–483)	308	0.211	2.7
Ni-P/MCM(1–663)	616	0.425	2.7
Ni-P/MCM(2–483)	214	0.138	2.6
Ni-P/MCM(2–663)	462	0.301	2.5
Ni-P/MCM(3–483)	83	0.042	2.0
Ni-P/MCM(3–663)	196	0.113	2.3

### 3.3. Textural properties

**Table 1** summarizes the textural properties of support and catalysts reduced at 493 and 583 K. The surface area and pore volume of the MCM-41 support are 1012 m<sup>2</sup> g<sup>-1</sup> and 0.816 cm<sup>3</sup> g<sup>-1</sup>, respectively. It can be seen that these catalysts suffer a loss of surface area and pore volume, especially the catalysts rich in phosphorus. This may be due to the formation of a phosphosilicate, which causes a shrinkage in the MCM-41 structure [36]. Abu et al. [37] have also found that metal phosphides supported on MCM-41 have much lower surface areas than pristine MCM-41, indicating that some of the MCM-41 structure is lost during the preparation of metal phosphide. Furthermore, **Table 1** shows the P content had significant effect on the surface area and pore volume. The surface area and pore volume decrease with decreasing of P contents, which can be contributed to the excess P evolved during the reduction covers on the outer surface of catalysts. For the catalysts with same initial P/Ni molar ratios, the catalysts reduced at 663 K have higher surface area than that of the catalysts reduced at 483 K. The low surface area of catalysts reduced at 483 K is attributed to the presence of un-reduced hypophosphites.

### 3.4. XPS

In order to gain further insight into the surface composition and the valence states of Ni<sub>2</sub>P, the XPS spectrum of MCM-41 supported Ni<sub>2</sub>P samples with initial P/Ni molar ratio of 1, 2 and 3 reduced at 483 and 663 K was obtained. **Table 2** shows the binding energy values and Ni/P and Ni/Si atomic ratios for all the samples.

For the Ni-P/MCM(X-663) catalysts, Ni 2p core level spectrum involves two contributions (**Fig. 3(a)**). The first is assigned to Ni<sup>δ+</sup> in Ni<sub>2</sub>P phase and centered at 852.6–853.5 eV [25], and the second at 856.4–857.3 eV, corresponding to the possible interaction of Ni<sup>2+</sup> ions with phosphate ions, as a consequence of a superficial passivation, along with the broad shake-up peak at approximately 6.0 eV higher than that of the Ni<sup>2+</sup> species [38]. This satellite peak is due to divalent species [39,40], although in the literature has also been assigned to trivalent and oxy-sulfided nickel species [29,41]. Other broad peaks, centered at high binding energy side, are assigned to the Ni 2p signal from oxidized Ni species [25]. Comparing contributions at 852.6–852.7 eV, we can see that the intensity of the Ni<sup>δ+</sup> is in the order Ni-P/MCM(2–663)>Ni-P/MCM(3–663)>Ni-P/MCM(1–663). The weakest contribution observed with Ni-P/MCM(1–663) is understandable, the lower P content in precursor leads to less Ni<sub>2</sub>P phase formed (**Fig. 2** XRD patterns, sample (b)). With P/Ni initial P/Ni molar ratio of and 3, P content in precursor is enough to formation of Ni<sub>2</sub>P, but the excess P covers on the outer surface of catalyst, and this will leads to influence the detection of Ni<sup>δ+</sup>. The binding energy for Ni 2p in the Ni<sub>2</sub>P phase is very close to that reported for Ni<sup>0</sup> species (852.0–853.0 eV) [39]. Meanwhile, with regards to P 2p binding energy, it has been reported to be 129.5 eV for P<sup>δ-</sup> on

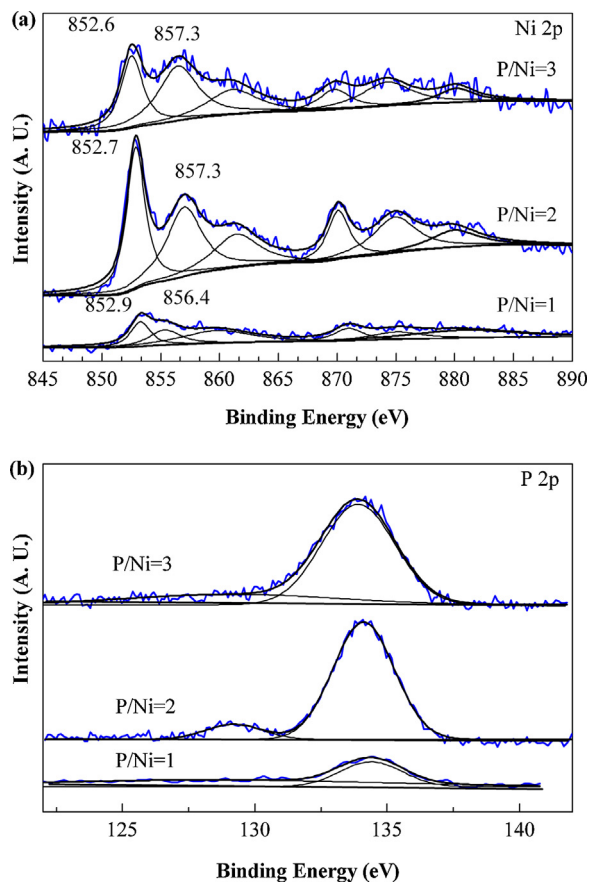


**Fig. 3.** XPS spectra of the Ni-P/MCM(X-663) with different initial P/Ni molar ratios.

bulk Ni<sub>2</sub>P and 133.5 for surface P<sup>5+</sup> (phosphate) due to the superficial oxidation of Ni<sub>2</sub>P particles [33]. As shown in the **Fig. 3(b)**, only the Ni-P/MCM(2–663) shows the P<sup>δ-</sup> band at 129.4 eV obviously, and the binding energy shifts lightly to a lower value, which indicates that there is an interaction between the Ni<sub>2</sub>P particles and the MCM-41 support. The Ni<sub>2</sub>P phase in sample of Ni-P/MCM(1–663) is too little that the P<sup>δ-</sup> is hardly observed. Because of the coverage of excess P on the surface, the sample of Ni-P/MCM(3–663) hardly exhibit the P<sup>δ-</sup> band. All the samples show the broad bands at 134–135 eV, which are assigned to P<sup>5+</sup> (phosphate) species [42], and which implies that there is a large amount of phosphate over the catalysts.

In order to investigate the Ni 2p and P 2p core level of the catalysts obtained at 483 K, the sample with initial P/Ni molar of 2 and 3 were considered. As shown in **Fig. 4(a)**, both the samples exhibit the Ni<sup>δ+</sup> and Ni<sup>2+</sup> species centered at 852.4–852.7 eV and 856.5–856.6 eV, respectively. However, the intensity of Ni<sup>δ+</sup> species bands of the catalysts reduced at 483 K is weaker than that of the catalysts reduced at 663 K (**Fig. 3(a)**), indicating a small amount of Ni<sub>2</sub>P is formed at 483 K. This conclusion could be confirmed by the results obtained by XRD, where the weak diffraction lines of Ni<sub>2</sub>P were observed. **Fig. 4(b)** shows P<sup>δ-</sup> is not observed in the two samples as was found in the catalyst Ni-P/MCM(2–663), while the P<sup>5+</sup> band at 134.6 eV remains, indicating phosphite ions are not totally reduced under the experimental conditions. Moreover, the P 2p signal centered at 133.0–133.7 eV, which is assigned to phosphorous in the form of HPO<sub>3</sub>H<sup>-</sup>, as previously reported by Infantes-Molina and Cecilia et al. [29,30]. This HPO<sub>3</sub>H<sup>-</sup> species is due to the disproportionation reaction of H<sub>2</sub>PO<sub>2</sub><sup>-</sup>.

XPS analyses were also used to calculate the surface P/Ni and Ni/Si atomic ratios (**Table 2**). If we consider the superficial

**Table 2**

Spectral parameters obtained by XPS analysis.

Sample	Binding energy (eV)					[0.8–9]Superficial atomic ratio	
	Ni 2p <sub>3/2</sub>		P 2p			P/Ni	Ni/Si
	Ni <sup>2+</sup>	Ni <sub>2</sub> P	PO <sub>4</sub> <sup>3-</sup>	HPO <sub>3</sub> H <sup>-</sup>	Ni <sub>2</sub> P		
Ni-P/MCM(1–663)	857.3	852.6	134.2	—	129.3	1.543	0.803
Ni-P/MCM(2–483)	856.6	852.4	134.7	133.0	129.3	5.618	0.057
Ni-P/MCM(2–663)	857.3	852.7	134.5	—	129.4	2.994	0.097
Ni-P/MCM(3–483)	856.5	852.7	134.6	133.6	129.2	6.098	0.053
Ni-P/MCM(3–663)	857.3	852.6	134.8	—	129.6	4.132	0.081

P/Ni atomic ratio, the theoretical ratio corresponding to precursor materials would be 1, 2, and 3, respectively. However, after reduction, these ratios increase considerably. This confirms that there is an enrichment of phosphorous on the surface of catalysts, although it is essentially present as PO<sub>4</sub><sup>3-</sup> forming a passivation layer in the surface of Ni<sub>2</sub>P [29]. Moreover, Table 2 also shows the P/Ni atomic ratios of Ni-P/MCM(2–483) and Ni-P/MCM(3–483), are higher than that of Ni-P/MCM(2–663) and Ni-P/MCM(3–663), respectively. This indicates that some phosphorous can be reduced at 663 K and partial loss of phosphorous due to the formation of PH<sub>3</sub> or P during reducing process [38]. As for the superficial Ni/Si atomic ratio, the Ni-P/MCM(2–483) and Ni-P/MCM(3–483) show the lowest Ni/Si atomic ratio, which may be due to the surface of catalysts are covered by excess phosphorous. The superficial Ni/Si atomic ratio of the catalysts obtained at 663 K is in the order Ni-P/MCM(2–663)>Ni-P/MCM(1–663)>Ni-P/MCM(3–663),

indicating phosphorous species in catalysts increases the dispersion of nickel on support [38,43].

### 3.5. CO uptake

CO uptake data measured at room temperature for the catalysts which obtained Ni<sub>2</sub>P phase was used to estimate the number of active sites, and the data is shown in Table 3. The CO uptake over the catalysts reduced at 663 K are in the order Ni-P/MCM(2–663)>Ni-P/MCM(3–663)>Ni-P/MCM(1–663). The lowest CO uptake over Ni-P/MCM(1–663) is easily accountable, because less active Ni<sub>2</sub>P phase was formed with the catalyst lower initial P/Ni molar ratio. The considerable lower CO uptake of Ni-P/MCM(3–663) catalyst indicate that excess P covers on the outer surface of the catalyst when the P/Ni molar ratio is higher, which led to the decrease in the amount of exposed nickel atoms used for adsorption of CO [38]. Although CO molecules may adsorb on P sites, their amount may be very small [44]. The possibility of the catalyst surface blocked by phosphate species for the samples rich in phosphorus is in accordance with BET and XPS results. The high CO uptake of Ni-P/MCM(2–663) also indicates that there are highly dispersed Ni<sub>2</sub>P particles in Ni-P/MCM(2–663). Moreover, compared with the Ni-P/MCM(2–663) and Ni-P/MCM(3–663) reduced at higher temperature, Ni-P/MCM(2–483) and Ni-P/MCM(3–483) show lower values of CO uptake, which may be due to the less Ni<sub>2</sub>P phase was reduced and the blocking by phosphate species at lower reduction temperature.

### 3.6. TEM

TEM images of the Ni-P/MCM(2–663) catalyst is shown in Fig. 5. The morphologies and particle sizes of the sample can be seen in the TEM images of Fig. 5(a). The Ni<sub>2</sub>P particle size ranged from approximately 6 to 18 nm, and which are homogeneously dispersed on the MCM-41 support. Unlike the typical stacked morphologies of Mo and W sulfides, Ni<sub>2</sub>P are not layered and form spherical particles that can be well dispersed on supports [45]. After reducing, the catalysts were subjected to a flow of a 0.5 vol.% O<sub>2</sub>/N<sub>2</sub> mixture at room temperature, so that a thin oxide layer formed on the outer surfaces of the particles, to prevent deep oxidation of the catalysts upon air exposure. Fig. 5(b) shows evidence of the passivation layer on a Ni<sub>2</sub>P particle in the Ni-P/MCM(2–663) catalyst. A light gray band with a thickness of approximately 1.5 nm can be seen to extend around the external edge of the Ni<sub>2</sub>P particle. This observation is consistent with the results reported by Sawhill et al. [46]. Fig. 5(c) shows the visible lattice spacing is about 0.22 nm, consistent with the d-spacing value for {111} crystallographic planes of the Ni<sub>2</sub>P phase.

### 3.7. The formation mechanism of Ni<sub>2</sub>P

To investigate the formation mechanism of the Ni<sub>2</sub>P prepared by this method, the analysis of the catalysts (initial P/Ni molar ratio

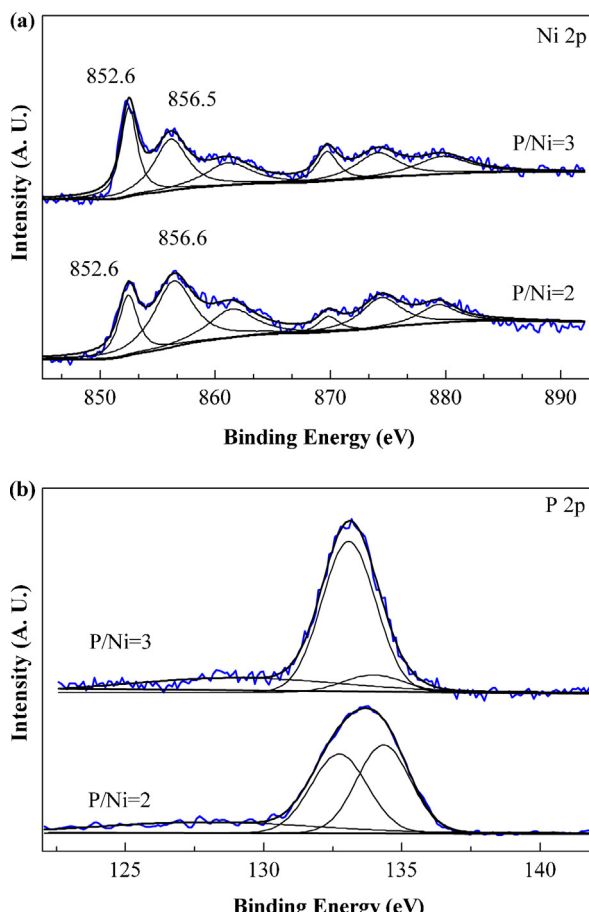
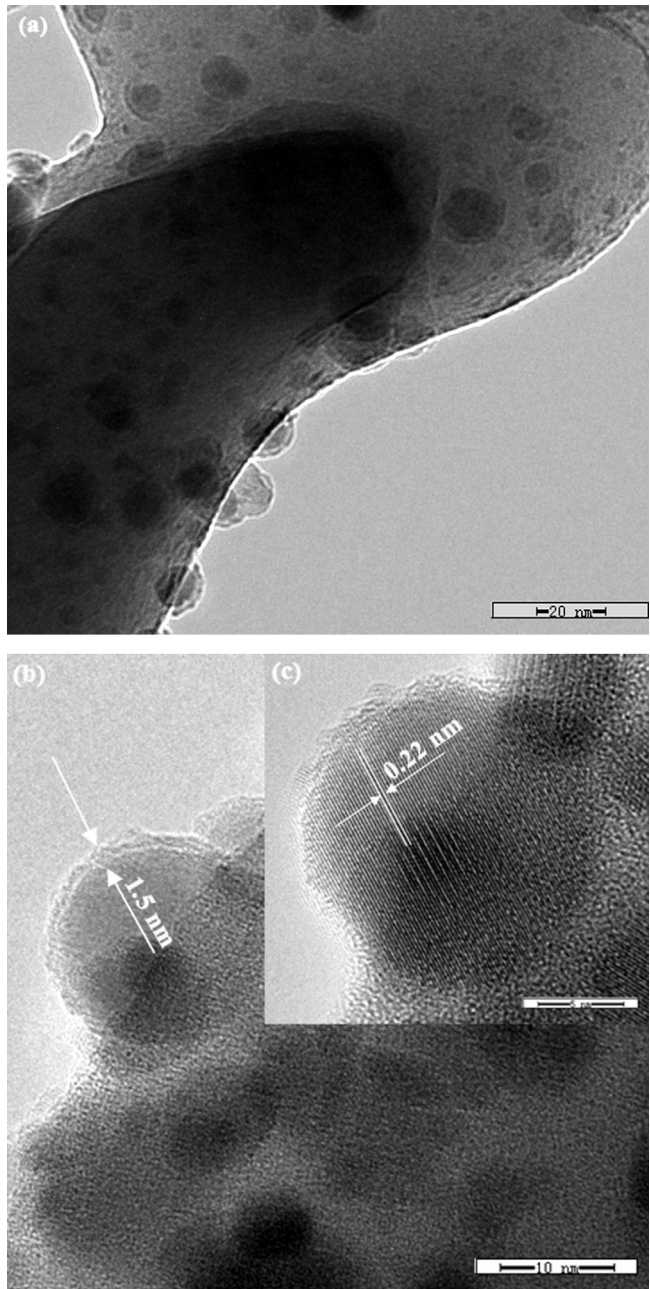


Fig. 4. XPS spectra of the Ni-P/MCM(X-483) with different initial P/Ni molar ratios.

**Table 3**CO uptake and DBT HDS performance over Ni<sub>2</sub>P catalysts.

Sample	Reaction temperature (K)	Conversion (%)	Selectivity (%)		CO uptake ( $\mu\text{mol g}^{-1}$ )	TOF ( $10^{-3} \text{s}^{-1}$ )
			BP	CHB		
Ni-P/MCM(1-663)	553	37.5	80.5	19.5	17	0.665
	573	42.8	83.8	16.2		0.759
	593	46.1	87.3	12.7		0.818
	613	50.0	90.1	9.9		0.887
	553	77.4	60.2	39.8		0.778
Ni-P/MCM(2-663)	573	83.2	65.5	34.5	30	0.836
	593	90.4	69.8	30.2		0.909
	663	99.9	72.3	27.7		1.004
	553	60.1	72.3	27.7		0.725
Ni-P/MCM(3-663)	573	67.5	78.8	22.2	25	0.814
	593	74.5	81.6	18.4		0.898
	613	83.1	85.6	14.4		1.002

**Fig. 5.** Low and high resolution TEM micrographs of the Ni-P/MCM(2-663) catalyst. (a) Low resolution TEM micrograph, (b) and (c) high resolution TEM micrographs.

of 2) obtained at different temperature and without passivating, as well as the precursor, are considered as representative (Fig. 6). Fig. 6(a) shows the corresponding Ni 2p core level spectrum of precursor and reduced sample, respectively. The precursor spectrum shows two Ni 2p<sub>3/2</sub> signals, one with a binding energy value of 856.3 eV which can be attributed to Ni<sup>2+</sup>, and another one of the broad shake-up satellite. This observation is in agreement with the results reported by Cecilia et al. [29]. The Ni 2p<sub>3/2</sub> signal for catalysts possess a small band located at about 852.7 eV, assigned to Ni<sup>δ+</sup> forming Ni<sub>2</sub>P. The Ni<sup>2+</sup> species can also be seen in the catalysts reduced at 483 and 593 K, but it can be hardly seen in the catalysts reduced at 663 K. Similarly, the P 2p signal for the precursor and the catalysts reduced at different temperature is shown in Fig. 6(b). If we consider the precursor spectra, the band centered at 132.7 eV can be assigned to phosphorous in the form of HPO<sub>2</sub><sup>-</sup>, and no high valence of phosphorous is observed, indicating the valence of phosphorous do not been modified during the preparation procedure. After reducing at 483 K, a small band at about 129.1 eV is observed, and which can be attributed to the P<sup>δ-</sup> forming Ni<sub>2</sub>P. Moreover, the bands at 133.6 and 134.8 eV appears in the catalyst reduced at 483 K, and which can be attributed to HPO<sub>3</sub>H<sup>-</sup> and PO<sub>4</sub><sup>3-</sup>, respectively [29]. When the reduction temperature rises up to 593 K, the band of PO<sub>4</sub><sup>3-</sup> is invisible, and the band of HPO<sub>3</sub>H<sup>-</sup> becomes weak, but the band of P<sup>δ-</sup> grows strong. This indicates that the HPO<sub>3</sub>H<sup>2-</sup> and PO<sub>4</sub><sup>3-</sup> species have been reduced to low valence of phosphorous (such as P<sup>δ-</sup> or other P species). With rising the reduction temperature up to 663 K, only the band of P<sup>δ-</sup> can be observed, indicating the HPO<sub>3</sub>H<sup>2-</sup> has been reduced completely.

In order to study the volatile species produced during the reduction process, we choose the activated carbon as the adsorbent to collect the effluent during reduction. The experimental configuration is shown in Fig. 7(a). After absorbing the effluent during reduction of catalysts reduced at 483, 593 and 663 K, the adsorbents were analyzed by the XPS to identify the elemental composition of the volatile products, and the result is shown in Fig. 7(b). It can be seen that oxygen (the binding energy of 533 eV) is observed in activated carbon for all the samples reduced at different temperature. It comes from the adsorbed O<sub>2</sub> or the adsorbed H<sub>2</sub>O. For catalyst reduced at 483 K, the phosphorous, chlorine and nitrogen elements can be observed at about 130, 200 and 400 eV, respectively, which indicates that the PH<sub>3</sub> (or P), HCl and NH<sub>3</sub> may be produced during the reduction process. It is worthwhile to note that the band of oxygen grows stronger after adsorption, implying the H<sub>2</sub>O is produced. With rising the reduction temperature up to 593 and 663 K, only the phosphorous and oxygen elements are still detected, indicating there is just reduction of phosphate and hypophosphate.

Guan et al. [24] have put forward the mechanism of the preparation of Ni<sub>2</sub>P catalysts by the heat treatment of a mixed salt precursor (NiCl<sub>2</sub> and NaH<sub>2</sub>PO<sub>2</sub>) in a static Ar protecting gas atmosphere. Our

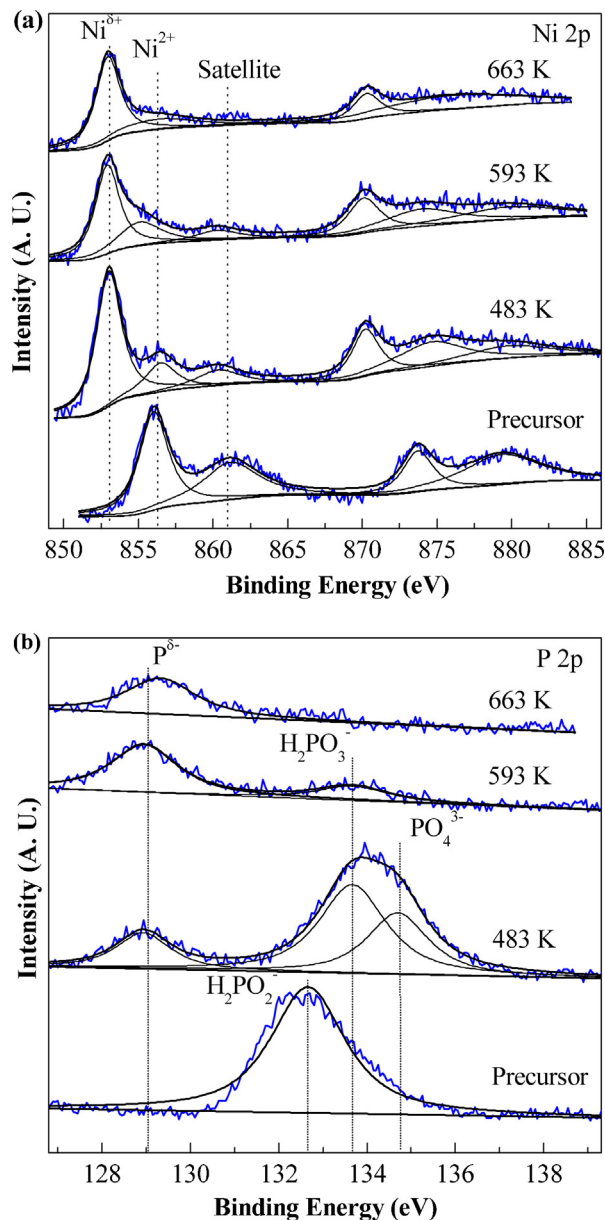


**Fig. 6.** XPS spectra of the Ni-P/MCM(2-Y) obtained at different temperature and without passivating.

research describes catalysts prepared in a flowing H<sub>2</sub> atmosphere. Thus, the formation process of Ni<sub>2</sub>P may be somewhat different from that reported by Guan et al. We propose that several possible reactions occur during the synthesis of Ni<sub>2</sub>P catalyst. The equations for the complete reaction would consist of three steps.

At the temperature of 483 K, the presence of some weak diffraction peaks of Ni<sub>2</sub>P (XRD analysis, Fig. 2(c)) and presence of the PH<sub>3</sub>, HCl and NH<sub>3</sub> (XPS analysis, Fig. 7(b)) indicate that the disproportionation reaction of NH<sub>4</sub>H<sub>2</sub>PO<sub>2</sub> can produce PH<sub>3</sub>, then the PH<sub>3</sub> reduces the NiCl<sub>2</sub> to Ni<sub>2</sub>P. However, this process is not the dominating reduction process. This is because the week peak of the P<sup>δ-</sup> forming Ni<sub>2</sub>P and large amounts of unreduced P species, such as HPO<sub>3</sub>H<sup>-</sup> and PO<sub>4</sub><sup>3-</sup>, can be observed from the XPS analysis of the catalyst reduced at 483 K and without passivation (Fig. 6(b)). Cecilia et al. [29] has found that the Ni(H<sub>2</sub>PO<sub>3</sub>)<sub>2</sub> was amorphous, but the Ni<sub>3</sub>(PO<sub>4</sub>)<sub>2</sub> can be detected by XRD. The XRD shows no other phase except Ni<sub>2</sub>P phase (Fig. 2(c)), confirming there is no Ni<sub>3</sub>(PO<sub>4</sub>)<sub>2</sub> formed. Therefore, it is reasonable to speculate that the

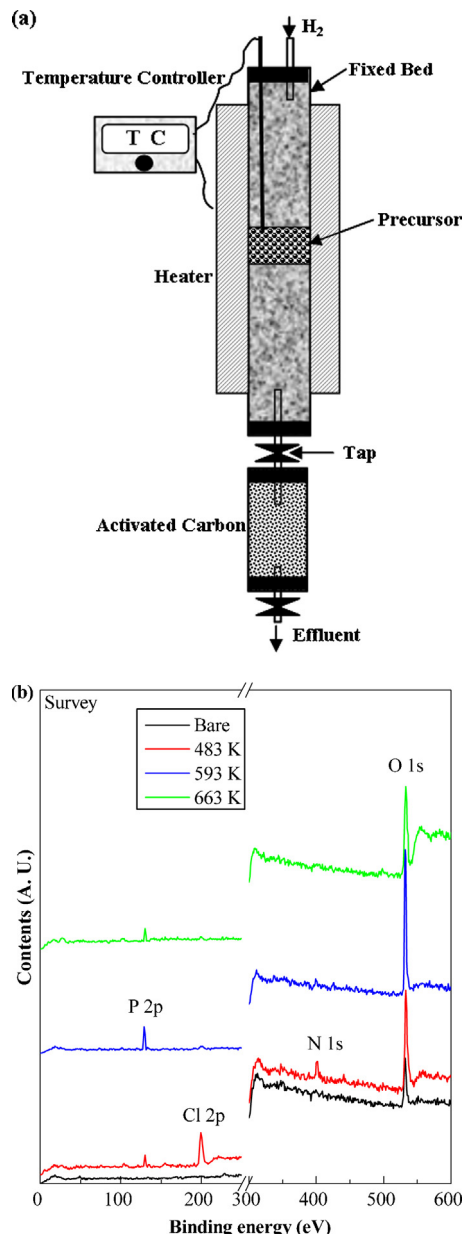
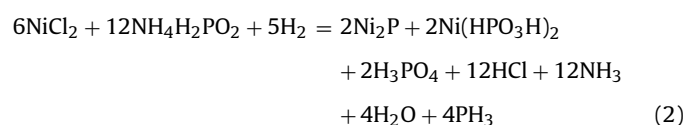


**Fig. 7.** The experimental configuration for gathering the volatile products (a) and the XPS results of the absorbed activated carbon (b).

Ni(HPO<sub>3</sub>H)<sub>2</sub> and H<sub>3</sub>PO<sub>4</sub> were formed during reduction at 483 K. The XPS (Fig. 7(b)) of absorbed activated carbon shows phosphorous, oxygen, chlorine and nitrogen elements confirms the formation of PH<sub>3</sub>, H<sub>2</sub>O, HCl and NH<sub>3</sub> at reduction temperature of 483 K. And the H<sub>2</sub>-TPR of NH<sub>4</sub>H<sub>2</sub>PO<sub>2</sub> shows a H<sub>2</sub> consumption peak at about 483 K indicates the H<sub>2</sub> (Fig. 1(f)) has also been involved at this temperature. In a word, the following reaction may describe the process occurred at reduction temperature of 483 K:



At the temperature of 593 K, the XRD analysis shows the crystallization of Ni<sub>2</sub>P grows stronger (Fig. 2(c)), and the XPS analysis of the catalyst reduced at 593 K and without passivation also shows a peak of the P<sup>δ-</sup> grows stronger (Fig. 6(b)), indicating more Ni<sub>2</sub>P were

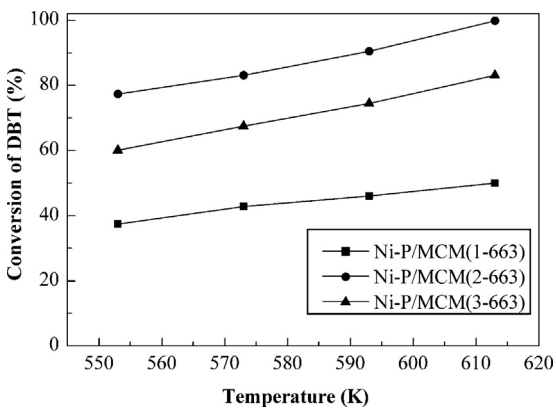
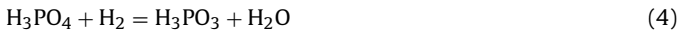
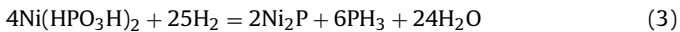


**Fig. 8.** The HDS activity of the catalysts with different initial Ni/P molar ratios. Pressure, 3.0 MPa; WHSV, 2 h<sup>-1</sup>; H<sub>2</sub>/oil ratio = 500 (V/V).

formed at this temperature than at 483 K. And the peak of PO<sub>4</sub><sup>3-</sup> disappeared and the band of HPO<sub>3</sub>H<sup>-</sup> became weak (Fig. 6(b)). The H<sub>2</sub>-TPR shows a marked H<sub>2</sub> consumption peak at this temperature indicates a reduction process occurred (Fig. 1(d)). The XPS of absorbed activated carbon (Fig. 7(b)) shows phosphorous and oxygen elements, this confirms the formation of PH<sub>3</sub> and H<sub>2</sub>O at this temperature. Infantes-Molina and Cecilia et al. [29,30] have also successfully prepared the Ni<sub>2</sub>P catalyst by H<sub>2</sub> reduction of a Ni(H<sub>2</sub>PO<sub>3</sub>)<sub>2</sub> precursor at 373–773 K. The reduction process occurred for 593 K through the following reaction, which can well coincide with the results showed by XRD and XPS that more Ni<sub>2</sub>P was formed at this temperature than 483 K:



Compared with the catalyst reduced at 593 K, the XRD shows the peaks intensities of Ni<sub>2</sub>P of catalyst reduced at 663 K remain unchanged (Fig. 2(c)), and the XPS also shows the P<sup>δ-</sup> peak intensity did not change (Fig. 6(b)) demonstrating no new Ni<sub>2</sub>P was formed. Moreover, only the P<sup>δ-</sup> can be observed from the XPS analysis indicating HPO<sub>3</sub>H<sup>-</sup> was completely reduced. The XPS of absorbed activated carbon (Fig. 7(b)) shows phosphorous and oxygen elements, indicates the formation of PH<sub>3</sub> and H<sub>2</sub>O during reduction. The H<sub>2</sub>-TPR shows a weak H<sub>2</sub> consumption peak confirms a reduction process occurred at 663 K (Fig. 1(d)). In conclusion, a reduction of H<sub>3</sub>PO<sub>3</sub> has occurred.



### 3.8. HDS performance

The above analysis shows the sample with initial P/Ni molar ratio of 1, 2 and 3 reduced at 663 K can be assigned to the Ni<sub>2</sub>P phase. To investigate their catalytic properties, the catalysts are evaluated by the HDS of DBT, and the result is shown in Fig. 8. In all cases, the conversion values increase gradually with the temperature. Comparing the three catalysts we can conclude that Ni-P/MCM(2-663) is more active than two other catalysts for HDS reaction, because Ni-P/MCM(2-663) shows higher conversion values in the temperature range of 280–340 K. The likely reason is that, with lower P content, such as the samples with P/Ni of 1, less Ni<sub>2</sub>P was formed (such as the XRD and XPS analysis). Nevertheless, at higher P content level, such as the samples with P/Ni of 3, excess P was formed on the catalyst surface, which resulted in the Ni<sub>2</sub>P active phase was blocked, and thus the catalyst shows low desulfurization activity.

The DBT conversion and CO uptake were used to calculate the HDS TOF for the catalysts. The HDS TOF of each catalyst increased

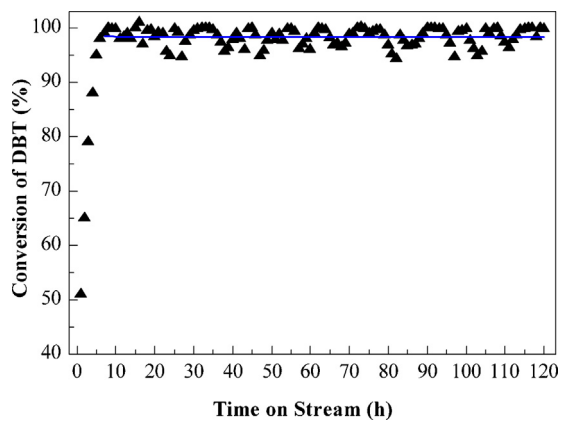


**Fig. 9.** Stability of HDS activity over the Ni-P/MCM(2-663) catalyst. Temperature, 613 K; pressure, 3.0 MPa; WHSV, 2 h<sup>-1</sup>; H<sub>2</sub>/oil ratio = 500 (V/V).

with temperature (Table 3), suggesting that the DBT HDS over Ni<sub>2</sub>P is a thermodynamically favorable reaction. Ni-P/MCM(2-663) possesses the highest TOF values what indicates a higher effectiveness of Ni<sub>2</sub>P phase on this sample. However, within the reaction temperature range of 593–613 K, the Ni-P/MCM(3-663) shows TOF values close to the Ni-P/MCM(2-663). It is possible that the sample lost some phosphorus during reaction, and the active sites covered by excess P were exposed again. Oyama et al. [38] have reported that the prolonged exposure of catalyst at the reaction temperature caused the Ni<sub>2</sub>P phase transform Ni<sub>12</sub>P<sub>5</sub> phase in the phosphorus deficient catalysts, which indicated that there was loss of phosphorus during the HDS reaction.

DBT undergoes HDS by two parallel pathways: the direct desulfurization (DDS) and the hydrogenation (HYD). DDS leads to the formation of biphenyl (BP), while HYD yields mainly cyclohexylbenzene (CHB) and small amount TH-DBT and HH-DBT. Because the transformation of BP to CHB is negligible in the presence of DBT, BP selectivity (SBP) is used as a measure of DDS pathway, and CHB represents the HYD pathway [47]. For Ni<sub>2</sub>P catalysts, the main products of HDS reaction were BP and CHB, hence the selectivity of reaction products can be calculated considering BP and CHB as the only products obtained. Table 3 illustrates the variations of BP and CHB yields with temperature over MCM-41 supported Ni<sub>2</sub>P obtained at 483 K and 663 K. It can be seen that BP is formed in greater proportions in all cases, with DDS being the favored reaction route. The yield of BP increased with temperature for each catalyst. The selectivity to CHB of Ni-P/MCM(2-663) is highest and that of other samples are lower. As reported by the literature [48], there are two types of sites in Ni<sub>2</sub>P, Ni(1) sites with tetrahedral coordination and Ni(2) sites with square pyramidal coordination, both Ni(1) and Ni(2) sites are present on large crystallites but that the Ni(2) sites are more numerous on the more highly dispersed samples. The lower coordination Ni(1) sites are responsible for desulfurization by the DDS pathway by taking on a sulfur atom while the Ni(2) sites are the high-activity sites that carry out HDS by the hydrogenation (HYD) route. Hence, we conclude that the acceleration of the HYD pathway over the catalysts must be associated with the dispersion of active phase. The Ni-P/MCM(2-663) catalyst has good dispersion (as the CO uptake analysis), this may lead to more Ni(2) sites and less steric hindrance during sulfur adsorption of reactants, resulting in a higher CHB selectivity.

Fig. 9 shows the results of Ni-P/MCM(2-663) catalyst stability for HDS of DBT within 120 h. It can be known from Fig. 9 that the activity of catalyst increases gradually in the initial 6 h, and the conversion of DBT close to 99% after 6 h and kept for 114 h without activity loss under the given reaction condition. The Ni-P/MCM(2-663) catalyst improves its catalytic capacity with initial

6 h, which suggests that there is a formation of an intermediate phase which is more active than Ni<sub>2</sub>P. The surface modification of Ni<sub>2</sub>P phase during the HDS reaction and the explanation of its excellent behavior with initial time on stream have been considered in the literature as consequence of the presence of a superficial phosphosulfide as active phase with a stoichiometry represented by NiP<sub>x</sub>S<sub>y</sub> [49,50]. In a recent study of Ni<sub>2</sub>P/SBA catalysts, Korányi et al. [42] reported that the presence of a superficial phosphosulfide with a composition Ni<sub>2.4</sub>P<sub>1.0</sub>S<sub>0.24</sub> is the real active phase of HDS reaction. Moreover, Ni<sub>2</sub>P has better sulfur resistance than metal carbides and nitrides which transform into metal sulfides with normal activity under HDS conditions [1], the conversion of DBT maintains at 99% in the case of DBT content in feed is as high as 1 wt% as shown in Fig. 9. Although the surface of Ni<sub>2</sub>P takes up sulfur atoms under HDS conditions, the kernel of the Ni<sub>2</sub>P particles remains intact [44,51,52].

#### 4. Conclusions

Ni<sub>2</sub>P catalysts were successfully prepared by H<sub>2</sub> reduction of a solid mixture of NH<sub>4</sub>H<sub>2</sub>PO<sub>2</sub> and NiCl<sub>2</sub>·6H<sub>2</sub>O precursor, and by using a silica mesoporous material such as MCM-41 as material support. This method is energy saving because of no need of calcination step and a low reduction temperature is required. Both the XRD and XPS analysis showed that the phosphorus content in precursor has an effect on the formation of the active phase. With sample of initial P/Ni molar ratio >0.5, the Ni<sub>2</sub>P was successfully obtained at lower reduction temperature, and a high initial P/Ni molar ratio favors the formation of Ni<sub>2</sub>P at lower temperature (483 K). Using of less oxidic phosphorus precursor of hypophosphite enabled the Ni<sub>2</sub>P to be formed at low reduction temperature. Ni<sub>2</sub>P catalysts prepared by this method proved to be highly active for DBT HDS. The stability of these catalysts is high, with no deactivation observed with 120 h time on stream whilst displaying an improved conversion of close to 99% with high selectivity of BP. The results suggest that this synthesis provides a potential new and general route for the preparation of supported Ni<sub>2</sub>P catalyst.

#### Acknowledgments

The authors acknowledge the financial supports from the National Natural Science Foundation of China (21276048), the Natural Science Foundation of Heilongjiang Province (ZD201201).

#### References

- [1] S.F. Yang, C.H. Liang, R. Prins, J. Catal. 237 (2006) 118–130.
- [2] C. Song, X. Ma, Appl. Catal. B: Environ. 41 (2003) 207–238.
- [3] K.H. Choi, N. Kunisada, Y. Korai, I. Mochida, K. Nakano, Catal. Today 86 (2003) 277–286.
- [4] S.K. Bej, S.K. Maity, U.T. Turaga, Fuel 18 (2004) 1227–1237.
- [5] X. Wang, P. Clark, S.T. Oyama, J. Catal. 208 (2002) 321–331.
- [6] S.T. Oyama, J. Catal. 216 (2003) 343–352.
- [7] S.T. Oyama, X. Wang, Y.K. Lee, W.J. Chun, J. Catal. 221 (2004) 263–273.
- [8] Y. Shu, Y.K. Lee, S.T. Oyama, J. Catal. 236 (2005) 112–121.
- [9] J. Guan, Y. Wang, M.L. Qin, Y. Yang, X. Li, A.J. Wang, J. Solid State Chem. 182 (2009) 1550–1551.
- [10] Y.Y. Shu, S. Ted Oyama, Carbon 43 (2005) 1518–1532.
- [11] G. Berhault, P. Afanasiev, H. Loboue, C. Geantet, T. Cseri, C. Pichon, C. Guillot Deudon, A. Lafond, Inorg. Chem. 48 (2009) 2985–2992.
- [12] M.S. Barry, E.G. Gillan, Chem. Mater. 20 (2008) 2618–2620.
- [13] S. Liu, X. Liu, L. Xu, Y. Qian, X. Ma, J. Cryst. Growth 304 (2007) 430–434.
- [14] H.L. Su, Y. Xie, B. Li, X.M. Liu, Y.T. Qian, Solid State Ionics 122 (1999) 157–160.
- [15] Z. Liu, X. Huang, Z. Zhu, J. Dai, Ceram. Int. 36 (2010) 1155–1158.
- [16] K.S. Cho, H.R. Seo, Y.K. Lee, Catal. Commun. 12 (2011) 470–474.
- [17] W.R.A.M. Robinson, J.N.M. Gestel, T.I. Korányi, S. Eijlsbouts, A.M. Kraan, J.A.R. Veen, V.H.J. Beer, J. Catal. 161 (1996) 539–550.
- [18] A.E. Henkes, R.E. Schaak, Chem. Mater. 19 (2007) 4234–4242.
- [19] Y. Chen, H. She, X. Luo, G.H. Yue, D.L. Peng, J. Cryst. Growth 311 (2009) 1229–1233.
- [20] X. Zheng, S. Yuan, Z. Tian, S. Yin, J. He, K. Liu, L. Liu, Mater. Lett. 63 (2009) 2283–2285.
- [21] J. Park, B. Koo, K.Y. Yoon, Y. Hwang, M. Kang, J.G. Park, T. Hyeon, J. Am. Chem. Soc. 127 (2005) 8433–8440.
- [22] H.R. Seo, K.S. Cho, Y.K. Lee, Mater. Sci. Eng. B 176 (2011) 132–140.
- [23] A.E. Henkes, Y. Vasquez, R.E. Schaak, J. Am. Chem. Soc. 129 (2007) 1896–1897.
- [24] Q.X. Guan, W. Li, M.H. Zhang, K.Y. Tao, J. Catal. 263 (2009) 1–3.
- [25] L. Song, S. Zhang, Q. Wei, Catal. Commun. 12 (2011) 1157–1160.
- [26] L. Song, S. Zhang, Powder Technol. 208 (2011) 713–716.
- [27] G. Shi, J. Shen, Catal. Commun. 10 (2009) 1693–1696.
- [28] Q. Guan, W. Li, J. Catal. 271 (2010) 413–415.
- [29] J.A. Cecilia, A. Infantes-Molina, E. Rodríguez-Castellón, A. Jiménez-López, J. Catal. 263 (2009) 4–15.
- [30] A. Infantes-Molina, J.A. Cecilia, B. Pawelec, J.L.G. Fierro, E. Rodríguez-Castellón, A. Jiménez-López, Appl. Catal. A 390 (2010) 253–263.
- [31] H.I. Meléndez-Ortiz, L.A. García-Cerda, Y. Olivares-Maldonado, G. Castruita, J.A. Mercado-Silva, Y.A. Perera-Mercado, Ceram. Int. 38 (2012) 6353–6358.
- [32] V. Teixeira da Silva, L.A. Sousa, R.M. Amorim, L. Andriani, S.J.A. Figueiroa, F.G. Requejo, F.C. Vicentini, J. Catal. 279 (2011) 88–102.
- [33] H. Song, M. Dai, Y.T. Guo, Y.J. Zhang, Fuel Process. Technol. 96 (2012) 228–236.
- [34] C. Stinner, R. Prins, T. Weber, J. Catal. 202 (2001) 187–194.
- [35] C. Stinner, Z. Tang, M. Haouas, Th. Weber, R. Prins, J. Catal. 208 (2002) 456–466.
- [36] V. Zuzaniuk, R. Prins, J. Catal. 219 (2003) 85–96.
- [37] I.I. Abu, K.J. Smith, Appl. Catal. A 328 (2007) 58–67.
- [38] S.T. Oyama, X. Wang, Y.K. Lee, K. Bando, F.G. Requejo, J. Catal. 210 (2002) 207–217.
- [39] D. Eliche-Quesada, J. Merida-Robles, P. Maireles-Torres, E. Rodriguez-Castellon, A. Jimenez-Lopez, Langmuir 19 (2003) 4985–4991.
- [40] J.N. Kuhn, N. Lakshminarayanan, U.S. Ozkan, J. Mol. Catal. A 282 (2008) 9–21.
- [41] N. Escalona, J. Ojeda, P. Baeza, R. Garcia, J.M. Palacios, J.L.G. Fierro, A.L. Agudo, F.J. Gil-Llambias, Appl. Catal. A 287 (2005) 47–53.
- [42] T.I. Korányi, Z. Vít, D.G. Poduval, R. Ryoo, H.S. Kim, E.J.M. Hensen, J. Catal. 253 (2008) 119–131.
- [43] T.L. Tarbuck, K.R. McCrea, J.W. Logan, J.L. Heiser, M.E. Bussell, J. Phys. Chem. B 102 (1998) 7845–7857.
- [44] K.A. Layman, M.E. Bussell, J. Phys. Chem. B 108 (2004) 10930–10941.
- [45] Y.K. Lee, Y. Shu, S.T. Oyama, Appl. Catal. A 322 (2007) 191–204.
- [46] S.J. Sawhill, K.A. Layman, D.R.V. Wyk, M.H. Engelhard, C. Wang, M.E. Bussell, J. Catal. 231 (2005) 300–313.
- [47] X. Li, Z.C. Sun, A.J. Wang, X.N. Yang, Y. Wang, Appl. Catal. A 417/418 (2012) 19–25.
- [48] S.T. Oyama, Y.K. Lee, J. Catal. 258 (2008) 395–399.
- [49] T. Kawai, K.K. Bando, Y.K. Lee, S.T. Oyama, W.J. Chun, K. Asakura, J. Catal. 241 (2006) 20–24.
- [50] A.E. Nelson, M. Sun, A.S.M. Junaid, J. Catal. 241 (2006) 180–188.
- [51] F. Sun, W. Wu, Z. Wu, J. Guo, Z. Wei, Y. Yang, Z. Jiang, F. Tian, C. Li, J. Catal. 228 (2004) 298–310.
- [52] Z.L. Wu, F.X. Sun, W.C. Wu, Z.C. Feng, C.H. Liang, Z.B. Wei, C. Li, J. Catal. 222 (2004) 41–52.